Pseudomorphic Inverted HEMT Suitable to Low Supplied Voltage Application

Masaaki Kasashima, Yukari Arai, Hiroki Inomata Fujishiro, Hiroshi Nakamua, and Seiji Nishi

Abstract—**Enhancement-mode pseudomorphic inverted HEMT with short gate length shows superior saturation properties in low drain voltage. Excellent saturation properties in the low field is suitable to low supplied voltage application. High frequency properties of FET were also studied by using two types of frequency dependent measurement systems which represent active load and common-source circuits. It was confirmed that the feature of low knee voltage in the static I–V is preserved above 100 kHz, which predicts the microwave characteristics of the device. The estimated output power for the device was 50% higher than that of conventional pseudomorphic HEMT at supplied voltage of 1 V.**

Introduction

RECENTLY, demands for low-voltage-operating high-speed devices are growing rapidly [1], [2], not only in digital application but also in analog/microwave applications. Low voltage operation is indispensable for reducing the power dissipation in applications for portable apparatus or to realize multi-cascoded circuits such as Gilbert cell multipliers which can be operated by a battery power supply.

Among various devices, submicron gate HEMT is reported [3] to be suitable for low voltage operating digital IC's. Especially, pseudomorphic inverted HEMT (P-I-HEMT) operates propagation delay time of 6.6 picosecond at room temperature under low supplied voltage of 0.9 V [4]. This data is one of the fastest ever reported. Furthermore, operating voltage is lower than any other devices. These results imply P-I-HEMT to be also suitable to low voltage operating microwave device. Saturation properties of P-I-HEMT under low supplied voltage were examined in detail by the second derivative of drain current with respect to drain voltage, and were compared with other devices and process conditions.

On the other hand, many papers have revealed that I–V properties of FETs in RF are different from those in dc [5], [6], and the real properties must be discussed in frequency region at least around 100 kHz or 1 MHz.

In this paper, we discuss the low voltage properties of P-I-HEMT in various frequency range and we show that the advantage of P-I-HEMT is maintained even in the RF. The measurement systems we employ here are to simulate two types of applications, switching transistor and active load transistor, in the frequency range up to 1 MHz.

Manuscript received July 10, 1992; revised July 30, 1992.
The authors are with Semiconductor Technology Laboratory, Oki Electric Industry Co., Ltd, 550-5 Higashiasakawa, Hachioji, Tokyo 193, Japan.
IEEE Log Number 9203712.

Saturation Property in Static I–V Curve

For the proper operation of FETs, the biasing in drain current saturated region is very important, therefore good saturation property in low field is indispensable for low voltage operation. We examined static curves in detail, especially the position and the shape of the knee.

Figs. 1 and 2 show the comparison in static properties between inverted HEMT (I-HEMT) and GaAs MESFET. They have 0.5 μm length, 10 μm width recessed gate structure and epitaxial layers grown by MBE. Their threshold voltages are -1.0 V. The I-HEMT structure, in which an undoped GaAs channel exists on an AlGaAs layer, has the advantage in the short gate length device, because of the superior confinement of the two-dimensional electron gas [7], [8]. It seems that the I-HEMT has lower knee voltage than MESFET, but the difference is not clear in simple I–V curves.

To examine more detailed knee properties, differential curves were delivered from these curves. Figs. 1(b) and 2(b) show derivatives of I_d curves i.e., drain conductances g_d versus drain voltages *Vd*. The g_d decreases in proportion to drain voltage Vd. In I-HEMT, the gradient of g_d versus Vd does not depend on Vg under the whole Vd region. Curves with different Vg values are almost parallel each other. On the contrary, the gradient of the MESFET becomes smaller as the Vg decreases. Figs. 1(c) and 2(c) show second derivatives, where vertical scales indicate absolute values. Difference of properties between the two devices becomes clear. In the second derivative curve of I_d, the peak position is thought to be the knee voltage, and the peak height and sharpness are thought to be the clearness of knee shape. In I-HEMT, when V_g decreases, curves shift to low field, but peak heights are not decreased so much. On the contrary, in case of MESFET, peak heights are decreased and the sharpness become reduced in low V_g region.

From the Figs. of 1 and 2, it is revealed that the I-HEMT structure has clearer knee shape and lower knee voltage than MESFET, and that the inverted HEMT structure is suitable to low supplied voltage application especially in low V_g region. It is considered that the I-HEMT has a smaller on-resistance because of its high electron mobility and it makes the knee voltage lower.

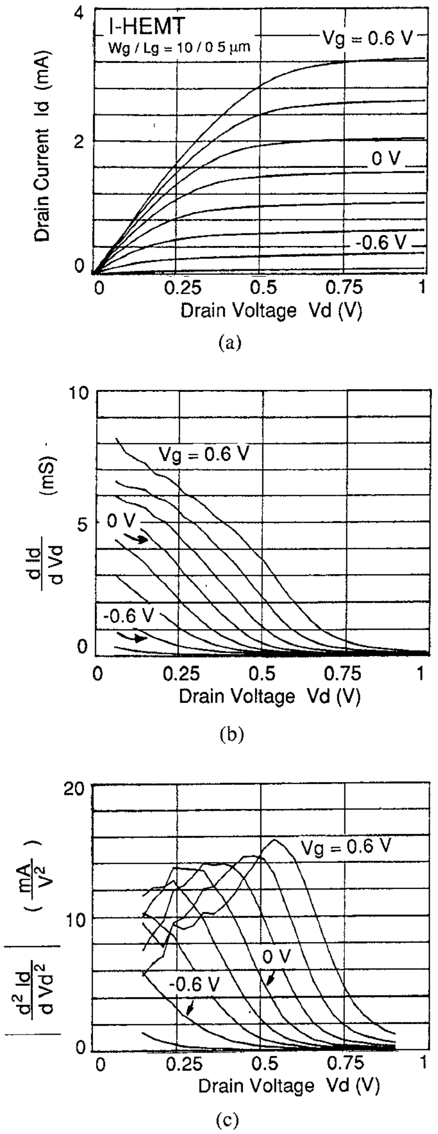

Fig. 1. Static characteristics of inverted HEMT. (a) I_d–V_d characteristics, (b) the derivative of drain current with respect to V_d (drain conductance) versus V_d, and (c) the second derivative of drain current versus V_d.

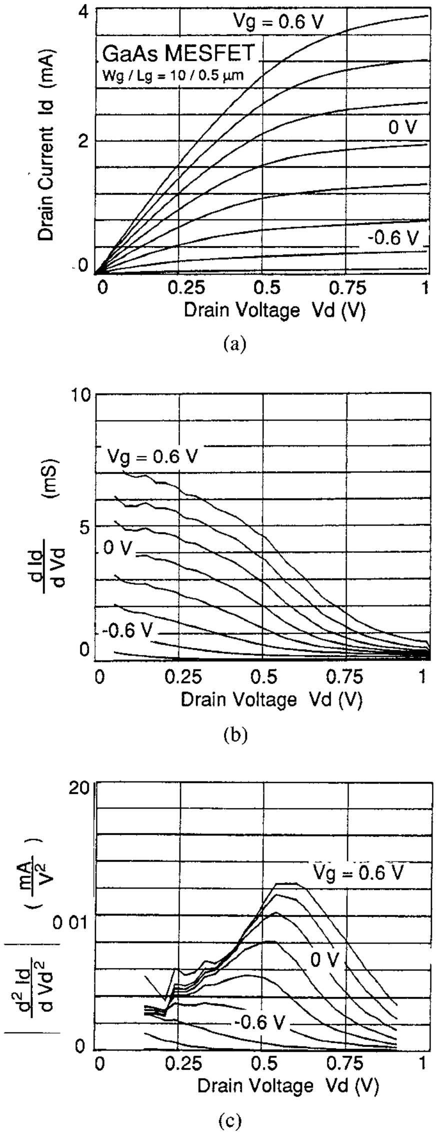

Fig. 2. Static characteristics of GaAs MESFET. (a) I_d–V_d characteristics, (b) the derivative of drain current with respect to V_d (drain conductance) versus V_d, and (c) the second derivative of drain current versus V_d.

By applying this evaluation method of knee properties to various kinds of devices, the following facts were revealed. 1) The short gate FET has lower knee voltage and clearer knee properties than the long gate FET, as long as strong short channel effects do not occur. It is considered that the shorter gate structure reduces the on resistor of FET channel and makes the knee voltage lower. 2) The knee voltage of the enhancement-mode I-HEMT is lower than that of the depletion-mode I-HEMT when compared in the V_g at maximum g_m. These results indicate that the enhancement-mode FET has an advantage of low voltage operation.

Device Structure and Characteristics

Based on the above-mentioned facts, it is considered that the superior durability against short channel effect and low on-resistance are indispensable for low voltage operating devices. Therefore, we employed two types of enhancement-mode very short gate HEMT structure devices which meet these requirements. One is a P-I-HEMT, and the other is a conventional structure well studied pseudomorphic HEMT (P-HEMT).

Pseudomorphic structure accomplishes improved transconductance (g_m) and reduced short channel effects due to high concentration and excellent confinement of two-dimensional electron gas in the InGaAs channel.

From now on, we compare the properties of P-I-HEMT and P-HEMT. Conventional HEMT structures (HEMT and P-HEMT) and also are suitable to inverted HEMT structures (I-HEMT and P-I-HEMT) to low voltage operation, compared to MESFET. However, the durability against short channel effects is larger in P-I-HEMT than in P-HEMT, and the g_m in enhancement-mode FET is larger in P-I-HEMT than in P-HEMT.

Fig. 3 shows the schematic cross-sectional figures of

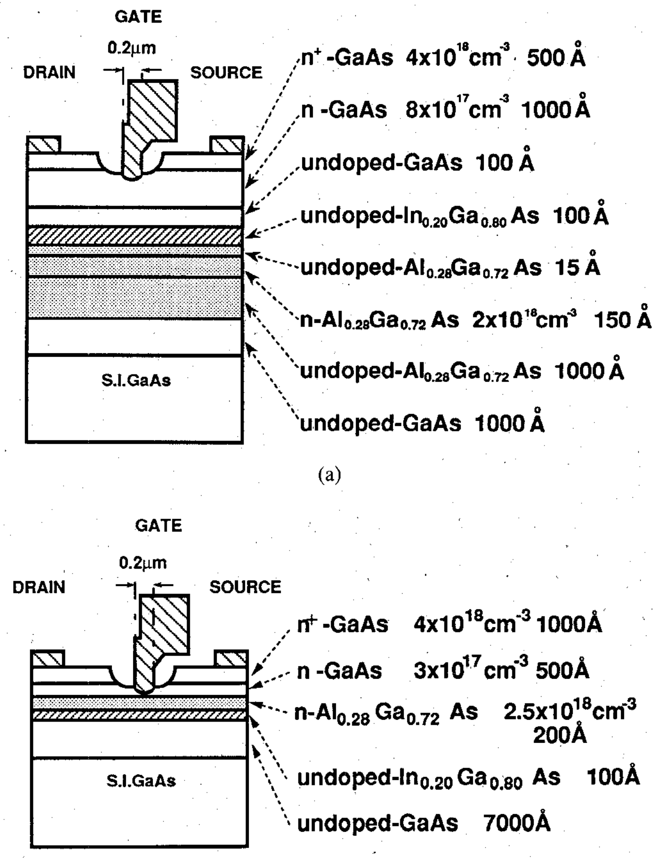

Fig. 3. Schematic cross section of (a) pseudomorphic inverted HEMT, and (b) pseudomorphic HEMT.

P-I-HEMT and P-HEMT. All the epitaxial layers are grown by MBE. In P-I-HEMT, pseudomorphic InGaAs channel layer is located on n-AlGaAs layer, opposite to P-HEMT structure. The inner part of the stepped recess region, formed by dry and wet two step etching, is filled with the 0.2 μm-long mushroom-shaped Ti/Al gate [9]. Both devices are fabricated in the same process lot, and in the completely same process conditions without etching depth.

Figs. 4 and 5 show static I–V properties and their second derivatives of enhancement-mode P-I-HEMT and P-HEMT. The gate length and width are 0.2 μm and 10 μm, respectively. As shown in I_d–V_d curves, P-I-HEMT has better drain current saturation properties and lower drain conductance compared with P-HEMT. In second derivative curves, their peak heights are higher than that for depletion-mode 0.5 μm gate I-HEMT (shown in Fig. 1(c)). P-I-HEMT shows much steeper and higher curves compared with P-HEMT.

Fig. 6 shows RF characteristics of 150 μm gate width P-I-HEMT and P-HEMT, measured by using microwave wafer probe head. The drain conductance under constant I_d of 20 mA is calculated from 0.5–12 GHz S-parameters. The maximum f_T in each V_d is also plotted. P-I-HEMT has smaller g_d in RF just as in dc. The maximum f_T of P-I-HEMT shows the largest value in as low drain voltage as 0.8 V.

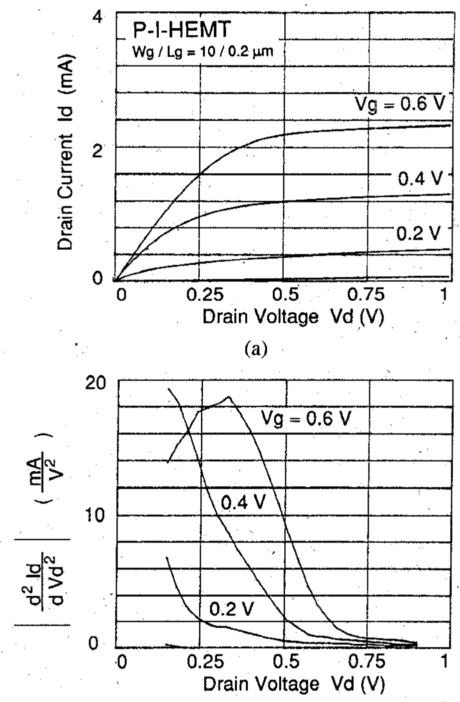

Fig. 4. Static characteristics of pseudomorphic inverted HEMT. (a) I_d–V_d characteristics, and (b) the second derivative of drain current with respect to V_d versus V_d.

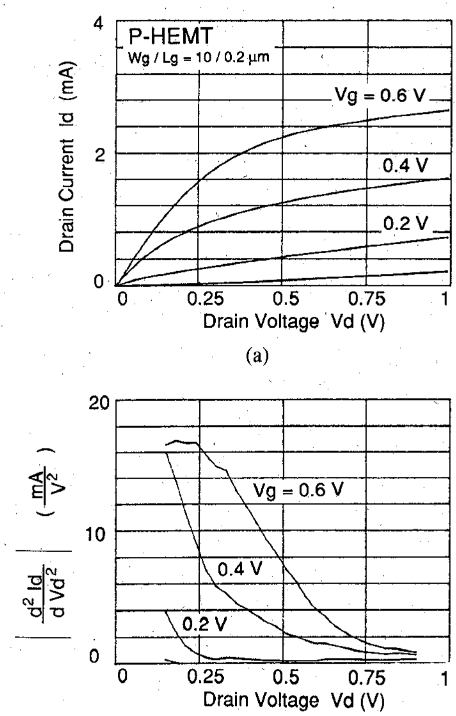

Fig. 5. Static characteristics of pseudomorphic HEMT. (a) I_d–V_d characteristics, and (b) the second derivative of drain current with respect to V_d versus V_d.

High Frequency I–V Measurement Systems

Most of the compound semiconductor FETs are known to show drastic changes of their characteristics around 100 Hz–10 kHz: such changes are related to deep level traps

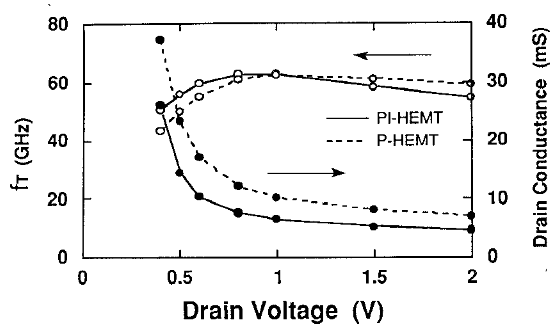

Fig. 6. Cut-off frequency and drain conductance calculated from 0.5–12 GHz S-parameters in P-HEMT and P-I-HEMT.

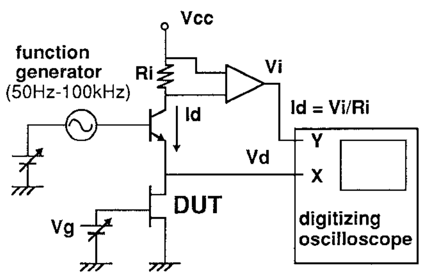

(a)

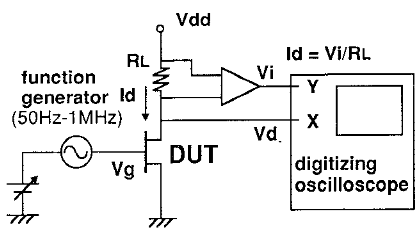

(b)

Fig. 7. Two types of frequency dependent measurement systems. (a) The system A which represent active load. (b) The system B which represent common-source circuit.

and make the RF device parameter like drain conductance quite different from the dc value. Consequently, parameters above 10 kHz, instead of dc data, will represent RF characteristics. Our interest was whether the good static I–V characteristics at low drain voltage is maintained in the RF condition, or not. The two kinds of measurement systems we employed are to show the RF I–V behavior of the devices.

Measurement system A is shown in Fig. 7(a). The bipolar transistor operates as an emitter follower circuit. The signal of function generator is applied to the base, and the drain voltage of DUT is applied from the emitter. The V_d can be swung as large as 5 $V_{p\text{-}p}$ up to 100 kHz under the constant gate voltage. The value of drain current is obtained from the potential difference of resistor R_i measured by the operational amplifier. I_d–V_d curves of the FET are obtained as the Lissajous's figure on the digitizing oscilloscope, and then averaging, smoothing and error-correction treatments are done by the computer. These I_d–V_d results are helpful to understand RF operation applied to active load and current source circuits.

In another system (system B: Fig. 7(b)), trapezoidal voltage up to 1 MHz is supplied to gate, and drain current is supplied through the load resistor R_L. This configuration gives the load lines of FETs on the digitizing oscilloscope, which are useful to common-source amplifier design.

Results and Discussion

Figs. 8 to 11 are I_d–V_d curves of 150 μm width gate P-I-HEMT measured by system A and/or B. Comparison of I_d–V_d curves under various measurement conditions are described as follows. Fig. 8 shows voltage swing and frequency dependences of I–V curves in P-I-HEMT measured by system A. In this figure, curves of 100 kHz with the amplitude from 0 V to 1, 2 and 4 V are plotted with the static curves of [50 Hz, 4 V]. In case of high frequency and large voltage swing such as the case of [100 kHz, 4 V], I_d decrease is serious in low V_d region. For smaller voltage swings of 1 $V_{p\text{-}p}$, the I_d decrease almost disappears.

The overlay plot I_d–V_d curves for 100 kHz with 0.6 V voltage swings around various bias points, are shown in Fig. 9. The center of each curve is exactly on the static or 50 Hz I–V curves, however, the fact that the gradient for 100 kHz is larger shows the frequency dispersion of g_d even in the small voltage swing around the operating points.

These results suggest that in the application of active load or current source circuit, frequency dispersion of g_d still remains even in the low supplied voltage conditions. However, when the voltage swing itself is small, the change in I_d is sufficiently suppressed.

Fig. 10 shows the result of P-I-HEMT measured by system B. Gate voltage is supplied from +0.6 V to below pinch-off voltage at 1 MHz. Several kinds of supplied voltages (from 0.5 V to 5 V by the step of 0.5 V) are applied, and several parallel load lines can be drawn. I–V curve (b) is obtained as an envelope of load line edges. Curve (a) is obtained by system A at 100 kHz, that is the same line as 4 $V_{p\text{-}p}$ condition in Fig. 8. Curve (c) is the static curve. In low frequency, curve (a) and (b) coincide with curve (c). In curve (b) measured by system B, although the drain current decreases in whole region, clear knee properties are not disappeared and the line is almost parallel to the static curve (c).

In Fig. 11, two kinds of load resistance (R_L = 15 Ω and 82 Ω) are compared at 1 MHz. The envelope of 82 Ω load line edge shows rounded curve at the knee, whereas that of 15 Ω load line has the clear knee. This fact suggests that the knee property in the RF I–V in the common-source amplifier application depends more on drain voltage swing than on gate voltage swing.

Fig. 12 shows the relation between output power and supplied voltage at the frequencies of 50 Hz and 1 MHz, where P-I-HEMT and P-HEMT are compared. Output power is obtained from power consumption of load resistor in measurement system B, and V_{dd} as shown in Fig. 7(b) gives supplied voltage. This estimation is equivalent

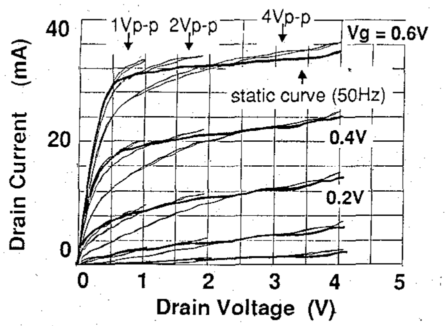

Fig. 8. Dependence of amplitude in large signal I–V characteristics (at 100 kHz) and static curve (at 50 Hz) of P-I-HEMT measured by system A.

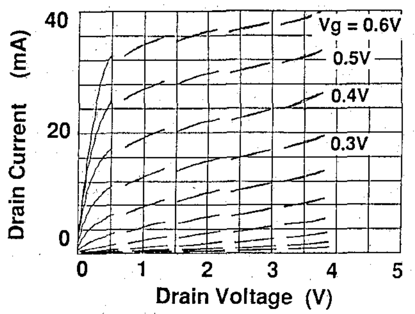

Fig. 9. I–V curves of P-I-HEMT for 100 kHz with 0.6 V voltage swing around various bias points measured by system A.

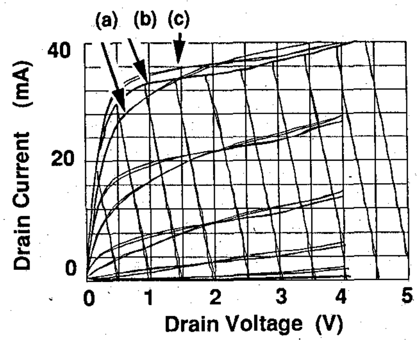

Fig. 10. Comparison of I–V curves for P-I-HEMT (a) measured by system A at 100 kHz, (b) measured by system B at 1MHz, and (c) the static curve.

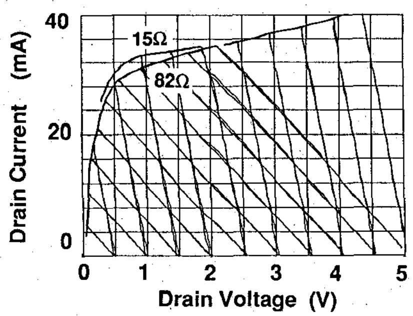

Fig. 11. Comparison of envelopes in measurement system B with load resistor of 15 Ω and 82 Ω.

to output power in RF without complex impedance matching problem, therefore, real device performance can be clarified. Solid lines and broken lines are for P-I-HEMT and P-HEMT, respectively. Open and closed circles show

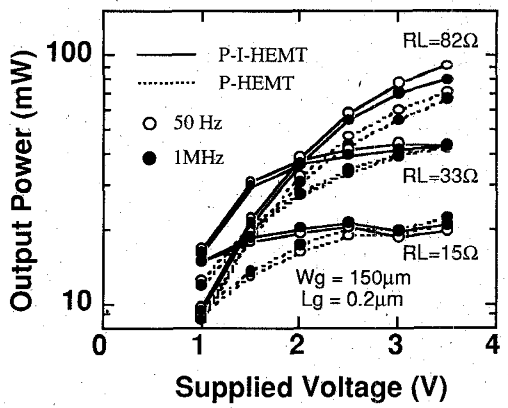

Fig. 12. Comparison of estimated output power versus supplied voltage between P-I-HEMT and P-HEMT as a parameter of R_L. Solid lines are for P-I-HEMT and broken lines are for P-HEMT. Open circles are measured at 50 Hz and closed circles are at 1 MHz.

the data at 50 Hz and 1 MHz, respectively. For small R_L, the degree of output power decrease as the supplied voltage (V_{dd}) decrease, is suppressed in P-I-HEMT compared with P-HEMT. For example, for $V_{dd} = 1$ V and $R_L = 15$ Ω, the output power of P-I-HEMT is 50% larger than that of P-HEMT as a typical data. Moreover, the frequency dispersion of power is small in the condition of low R_L and low V_{dd}. Large difference in power between 50 Hz and 1 MHz at $V_{dd} > 3$ V and $R_L = 82$ Ω is caused by the difference in the knee properties shown in Fig. 11.

From the result of the measurement with the system B, which represents the case of common-source power amplifier application, it is proved that frequency dispersion in power property is not serious for low supplied voltage operation. The excellent feature of low knee voltage in P-I-HEMT maintains even in the high frequency. The high output power of P-I-HEMT at low supplied voltage may be brought about by this low knee voltage.

Conclusion

In this paper, the properties of pseudomorphic inverted HEMT (P-I-HEMT) as a low-voltage-operating device is discussed.

First, static low field saturation properties are compared in detail between I-HEMT and GaAs MESFET, and it was revealed that the I-HEMT structure has a superior saturation property in low V_d and low V_g region.

To study the high frequency I–V properties of FET, two types of frequency dependent measurement systems which represent active load and common-source amplifier circuits were employed.

It was confirmed that the feature of low knee voltage in static I–V of P-I-HEMT is preserved above 100 kHz, which predicts the microwave characteristics of the device. Higher output power is obtained in P-I-HEMT than in P-HEMT at low supplied voltage. It is concluded that the enhancement-mode short gate length P-I-HEMT is one of the most promising devices which operates under very low supplied voltage.

Acknowledgment

The authors would like to acknowledge Dr. M. Sakuta, Mr. Y. Sato, and Mr. S. Takahashi for their encouragement during this study. They also thank Mr. K. Ohmuro and Mr. M. Itoh for valuable discussions and for supplying test devices.

References

[1] A. Shida, M. Kagamihara, M. Komatsu, and K. Kumagai, M. Hirata, "3.3 V BINMOS technology using NPN transistors without buried layers," in *IEEE IEDM Tech. Dig.*, 1991, pp. 431–434.

[2] R. A. Kiehl, J. Yates, L. F. Palmateer, S. L. Wright, D. J. Frank, T. N. Jackson, J. F. Degelormo, and A. J. Fleischman, "High-speed low-voltage complementary heterostructure FET circuit technology," in *IEEE GaAs IC Symp. Tech. Dig.*, 1991, pp. 101–104.

[3] M. Suzuki, S. Notomi, M. Ono, N. Kobayashi, E. Mitani, K. Odani, T. Mimura, and M. Abe, "A 1.2-ns HEMT 64-kb SRAM," *IEEE J. Solid-State Circuits*, vol. 26, no. 11, p. 1571–1576, Nov. 1991.

[4] H. Tsuji, H. I. Fujishiro, M. Shikata, K. Tanaka, and S. Nishi, "0.2μm gate pseudomorphic inverted HEMT for high speed digital IC's," in *IEEE GaAs IC Symp. Tech. Dig.*, 1991, pp. 113–116.

[5] A. Platzker, A. Palevsky, S. Nash, W. Strube, and Y. Tajima, "Characterization of GaAs devices by a versatile pulsed I–V measurement system," in *IEEE MTT-S Int. Microwave Symp. Dig.*, 1990, pp. 1137–1140.

[6] Y. Arai, M. Kasashima, N. Kobayashi, H. I. Fujishiro, H. Nakamura, and S. Nishi, "Characterization of anomalous frequency dispersion in GaAs BP-MESFETs by direct large-signal I–V measurement," *Inst. Phys. Conf. Ser. No. 120: Int. Symp. GaAs and Related Compounds*, Seattle, 1991, pp. 125–130.

[7] H. I. Fujishiro, H. Tsuji, and S. Nishi, "0.2μm gate pseudomorphic InGaAs/AlGaAs inverted HEMTs," *Inst. Phys. Conf. Ser. No. 112: Int. Symp. GaAs and Related Compounds*, 1990, pp. 453–458.

[8] H. I. Fujishiro, H. Tsuji, and S. Nishi, "Characterization of ultrahigh-speed pseudomorphic InGaAs/AlGaAs inverted high electron mobility transistors," *Japan J. Appl. Phys.*, to be published.

[9] K. Ohmuro, H. I. Fujishiro, M. Itoh, N. Nakamura, and S. Nishi, "Enhancement-mode pseudomorphic inverted HEMT for low noise amplifier," *IEEE Trans. Microwave Theory Tech.*, vol. 39, no. 12, pp. 1995–2000, Dec. 1991.

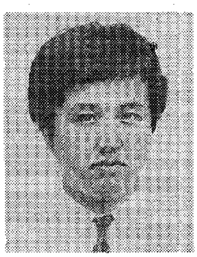

Masaaki Kasashima was born in Tokyo, Japan, on November 11, 1959. He received the B.E. and M.E. degrees in electronic engineering from Nihon University, Tokyo, in 1983 and 1985 respectively.

He then joined Oki Electric Industry Company, Ltd., Tokyo. He is currently engaged in the microwave GaAs IC technologies.

Mr. Kasashima is a member of the Japan Society of Applied Physics.

Yukari Arai was born in Tokyo, Japan, on April 12, 1962. She received the B.S. and M.S. degrees from the University of Tokyo, Tokyo, in 1986 and 1988, respectively.

In 1988, she joined Oki Electric Industry Company, Ltd., as a research staff of the Semiconductor Technology Laboratories. Since then, she has been working on processing technologies for compound semiconductor devices, especially MBE-grown HEMTs and MESFETs.

Ms. Arai is a member of the Japan Society of Applied Physics.

Hiroki Inomata Fujishiro was born in Kanagawa, Japan, on September 30, 1959. He received the B.S. and M.S. degrees in physics from the Science University of Tokyo, in 1982 and 1984, respectively.

In 1984, he joined the Research Laboratory, Oki Electric Industry Company, Ltd., where he has been engaged in the research and development of MBE growth of compound semiconductors and device technology for heterostructure FET's.

Mr. Fujishiro is a member of the Japan Society of Applied Physics.

Hiroshi Nakamura was born in Fukuoka, Japan, on Oct. 13, 1954. He received the B.E., and M.E., and Ph.D. degrees in electronic engineering from the University of Tokyo, Japan, in 1977, 1979, and 1982, respectively. He then joined Oki Electric Industry Company, Ltd. He is currently engaged in the microwave GaAs IC technologies.

Dr. Nakamura is a member of the Japan Society of Applied Physics and the Institute of Electronics, Information and Communication Engineers of Japan.

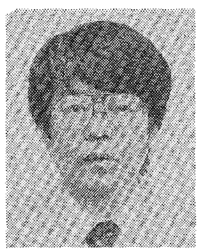

Seiji Nishi was born in Kanagawa, Japan, on April 18, 1950. He received the B.S., M.S., and Ph.D. degrees in physics from Osaka University, Japan, in 1974, 1976, and 1979, respectively.

In 1979, he joined the Research Laboratory, Oki Electric Industry Company, Ltd. He is currently engaged in research and development of MBE growth and HEMT devices.

Dr. Nishi is a member of the Japan Society of Applied Physics, and Institute of Electronics, Information and Communication Engineers of Japan.